Towards the Control of a Permanent Magnet Contactor Based on Charging and Recharging Techniques

CHIEH-TSUNG CHI
Department of Electrical Engineering
Chienkuo Technology University
No. 1, Chieh Shou N. Rd., Changhua City 500, Taiwan, R.O.C.
E-mail: jih@cc.ctu.edu.tw

Abstract: - This paper presents the design and analysis of a newly actuator with hardware based electronic control unit (ECU) for the control of energy dissipation in ac permanent magnet (PM) contactor. By using charging and recharging techniques, the making and breaking operations of contactor are controlled by ECU. In typical application where the gate driving signals of the closing and the opening power MOSFETs are limited to be produced during the closing and opening processes. In theory, no input electrical energy will be dissipated in the ac PM contactor during holding stage. Crucial to the design of the ECU is that has several outstanding benefits, such as simplicity, low cost, no noise pollution, energy saving and no voltage-sags affections. This paper describes the designing considerations for such a newly proposed ECU for use in a 220 V contactor control. Tests on experimental and simulation results illustrate the characteristic behaviors of the ac PM during making and breaking courses, and comparison evaluations of the energy-saving performance over a time interval between conventional ac electromagnetic (EM) contactor and proposed ac PM contactor.

Key-Words: - Electronic control unit (ECU), ac permanent magnet (PM) contactor, energy saving, no noise pollution, ac electromagnetic (EM) contactor.

1 Introduction

In the last two decades, a growing fields of research in contactor resulting in the development of a variety of prototypes [1-7]. In the control engineering and power distribution system, contactors are often used to control the voltage source of load by using breaking and making operations. They have been widely in many application fields. As the development of industry, they are increasingly used. If the running time is prolonged, of course, the conventional ac electromagnetic (EM) contactor consumes much more electrical energy to hold the armature in the closing state. In addition, the low voltage of the external ac voltage source appears in each of the power cycle leads to the air noise pollution of the environment. The contactor coil is easy to be burnt due to continual working state. To overcome the mentioned above critical drawbacks accompanies the conventional ac EM contactor, mechanical modifications of the conventional EM contactor are needed, such that arranges a permanent magnet on the armature and adds a newly proposed actuator including an ECU aims at the control of the contactor operation.

In recent years, many studies related to the dynamic characteristics of conventional ac EM contactor have been investigated by lots of authors. Numerous valuable researching results [5,8-10] were presented. For example, Nouri et al. proposed the bounce duration after contacts closing is significantly caused by the kinetic energy of the armature before two contacts impact in 1997. Therefore, in order to minimize the bounce duration, they presented that the kinetic energy in armature should be controlled as small as possible before two contacts impact or maximize the rate of dissipation after two contacts impact. The objective of them was achieved by timing coil energizing periods [4,6,11-15]. For completing the same objective, there were several similar manners have been published, such that selects a optimal closing phase angle of the external ac voltage source on purpose [7,16], closes and opens the contactor's contacts at the zero crossing points of load current [14,17] and so forth.

While many researchers aim at developing and analyzing the other new types of actuator for an ac contactor has attracted more and more attention, little work has been paid to the development of the ac PM contactors and their control circuits [18,19].

Hence, the purpose of this paper is to design a new hardware based actuator with the use of electronic control circuit. The most contributions for the new ac PM contactor including the proposed actuator are cost-effective, noise-free and high energy-saving performance. Not only does the mechanism of new ac PM contactor be described, but also the completed schematic diagram with ECU is also illustrated. Each part of circuit in ECU will be examined and its operation principle is explained as well. The proposed ECU has a variety of types of the applied voltage source, such as dc, ac and dc/ac voltage source. Simultaneously, it has a wide range of allowable voltage-source upper and lower limitations. The result of this study may be of interest to designers attempting to develop any type of control circuit for a new ac PM contactor; in particular, the energy-saving performance is taken as the most important consideration.

2 Mechanism of the Proposed Permanent Magnet Contactor

Fig. 1 shows the mechanisms of a conventional ac EM contactor and a proposed ac PM contactor. Obviously, the basic structure between ac EM contactor and ac PM contactor is same. As shown in Fig. 1(a), the making and breaking operations of the conventional ac EM contactor are controlled by using a mechanical switch SW. In contrast, Fig. 1(b) shows that an electronic control unit (ECU) is connected with the contactor body and the mechanical switch in series. According to the value of the external ac voltage source, the making and breaking operations of the ac PM contactor are controlled by the ECU. Comparing the configured appearance with each other, as a result of an ECU should be included in the ac PM contactor mechanism, thus, and leads to the increase in final manufacturing cost of contactor. However, the characteristic behaviors of ac PM contactor are exactly improved greatly, such that consumes little electric energy, avoid noise pollution at lower voltage, and removes the voltage-sags affections. In particular, regarding the energy-saving performance is superior to the other types of contactors.

Fig. 2 illustrates the functional block diagram of the ECU shown in Fig. 1(b). Highlights on attention to the capacitor C, it is made of electrolytic material. It is connected with the coil of the contactor in series. By energizing the power MOSFETs M1 and M2, the voltage across the capacitor C will be charged through diode D_1 and recharged directly, with regard to the making and breaking courses of ac PM contactor are then to be achieved.

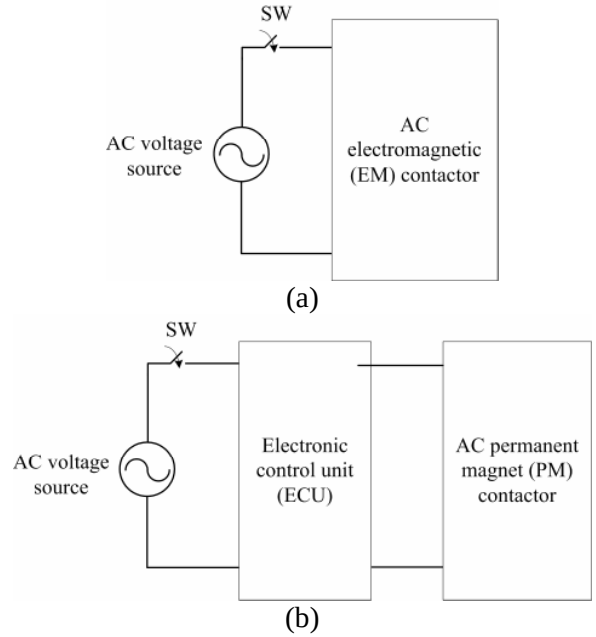

Fig. 1. Sketches the mechanisms: (a) conventional ac EM contactor; (b) proposed ac PM contactor.

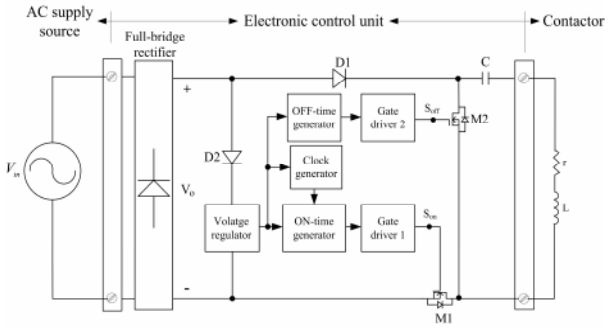

Fig. 2. Sketches the functional block diagram of ECU.

3 Mathematical models

The configuration of a typical newly proposed ac PM contactor is shown in Fig. 3 indicates that it includes three subsystems: an electrical system, a magnetic energy-conversion system, and a mechanical system. Like the conventional ac EM contactor, the objective of this type of ac PM contactor is to do the energy transfer from the electrical system to the mechanical system for the translational motion. Let the copper losses in the winding, the core losses in the iron, and the frictional losses in the armature be accounted for externally. The balance of energy flow over a period of time dt when the armature moves by dx, the energy transfer among this contactor can be expressed as

$$eidt = F_e dx + dW_f \quad (1)$$

The term in the left side of (1) is the electrical input energy, the first term in the right side of (1) is the mechanical output energy and while the second term in the right side of (1) is the change in the coupling field energy.

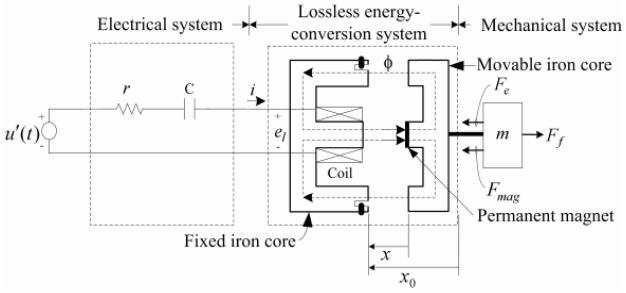

Fig. 3. Sketches the configuration of the developed ac PM contactor.

3.1 Electrical Model.

The electrical system shown in Fig. 3 can be simply represented by a voltage source $u(t)$, a resistor r, an electrolytic capacitor C and the voltage drop across the coil e_l. The dynamic behavior of the electrical system here can be described as an electric equation by employing the Kirchihoff's voltage law and shown below:

$$\begin{aligned} u'(t) &= ir + \frac{1}{C}\int idt + e_l \\ &= \left|\sqrt{2}U_{rms}\sin(wt)\right| \\ &= \sqrt{2}U_{rms}\sin(wt) \ , 2n\pi \le wt \le (2n+1)\pi \ , n = 0,1,2,.... \end{aligned} \quad (2)$$

where the ac voltage is assumed to be applied an ac sinusoidal voltage and is rectified by a full-wave rectifier. The second term in the right side of (2) is the charged or recharged voltage across the capacitor C. e_l is the voltage drop across the coil, it is equivalent to the derivative of the flux linkage with respect to time $d\lambda/dt$. In general, the flux linkage λ can be expressed as $\lambda = L(x)i$. above relevant relationship are substituted into (2) and yields

$$u'(t) = ir + L(x)\frac{di}{dt} + iv\frac{dL(x)}{dx} + \frac{1}{C}\int idt \quad (3)$$

where the moving velocity of armature is defined as the derivative of armature displacement, that is $v = dx/dt$. The term $L\,di/dt$ is the induced self-inductance voltage term, and the later term $iv(dL/dx)$ is the velocity-voltage term, in fact, which is responsible for the energy transfer from the electrical system to the magnetic energy-conversion system. During closing process, the power MOSFET M1 is switched on, rectified dc voltage $u'(t)$, capacitor C, the resistance included in the coil and conductors, and the coil inductance form an equivalent electric circuit of the electrical system, as seen in Fig. 4(a). The current i_1 flow through the contactor coil is used to produce an electromagnetic force and is integrated with the holding force with permanent magnet to overcome the spring anti-force. In contrast, during opening process, the power MOSFET M2 is conducted. The equivalent circuit of the electrical system shown in Fig. 4(b) is also a series RLC circuit, but the voltage source of the equivalent circuit is the reserved dc voltage across the breaking capacitor C, V_{co}. The current i_2 flows through the contactor coil and in the reverse direction. A reverse electromagnetic force is produced to counteract the holding force of permanent magnet. The remaining magnetic force is used to assist with the spring tension force for the purpose of quickly opening the contactor.

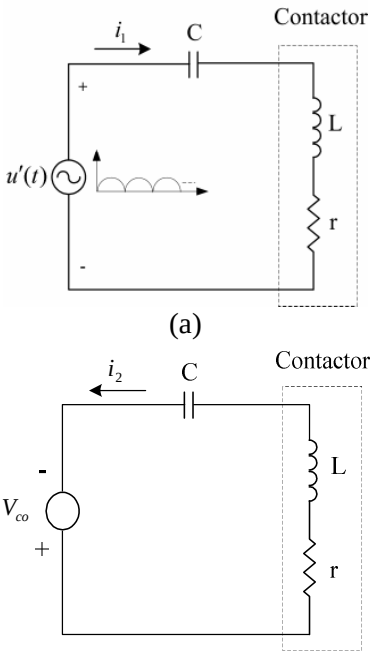

Fig. 4. Equivalent electric system: (a) during closing process; (b) during opening process.

3.2 Energy and Coenergy

If replacing the induced voltage e_l with $d\lambda/dt$ and rearranging the energy relationship between

subsystems as shown in (1), the change in magnetic field energy over the same time interval is given by

$$dW_f = id\lambda - F_e dx \tag{5}$$

Equation (5) depicts that the field energy stored is a function of λ and x. It is convenient to neglect all losses associated with the electrical system and magnetic fields, the fields are assumed to be conservative and lossless. In fact, almost all of the energy stored in the coupling fields is stored in the air gaps of the magnetic circuit of contactor. Owing to air is a conservative medium, all of the energy stored can be returned to the electrical or mechanical systems. The energy stored in a conservative field is a function of system variables and not the manner in which the variables reached that state. In other words, W_f is the same independent of how λ and x are brought to their final values. With the displacement of armature to be held fixed the energy stored in the coupling fields during the excitation of the electrical systems is equal to the energy supplied from the electrical system may be expressed as

$$W_f = \int id\lambda \tag{6}$$

The $\lambda - i$ curve of contactor is commonly a function of x. Thus, the stored energy is a function of λ and x. The total differential of $W_f(\lambda, x)$ with respect to the independent variable can be written

$$dW_f(\lambda, x) = \frac{\partial W_f}{\partial \lambda} d\lambda + \frac{\partial W_f}{\partial x} dx \tag{7}$$

Equating the coefficients of the $d\lambda$ and dx terms in (5) with those in (7), we derive

$$F_e = -\frac{\partial W_f}{\partial x} \tag{8}$$

In general, it is easier to hold the exciting current i rather than the flux linkage λ constant. In addition to the area which is enclosed by the λ axis and $\lambda - i$ curve, the complementary area which is enclosed by i axis and $\lambda - i$ curve is called the coenergy W_c, and it can be represented by

$$W_c = i\lambda - W_f(\lambda, x) \tag{9}$$

Taking the total derivative of (9), and replacing the $d(i\lambda)$ term on the right by $id\lambda + \lambda di$ and dW_f by the right side of (5), we obtain

$$dW_c = \lambda di + F_e dx \tag{10}$$

We note that the coenergy is a function of i and x. This is evident from the area of W_c being bounded by i and $\lambda - i$ curve which depends upon x. Equating the coefficients of the $d\lambda$ and dx terms in (5) with those in (10), we obtain

$$F_e = \frac{\partial W_c}{\partial x} \tag{11}$$

However, the developed electromagnetic force is determined by (8) or (11) is always in the direction of coordinate x as a direct result of the change in energy to mechanical system, that is the second term of (5). The electromagnetic force acts in such a direction to decrease stored energy for constant flux linkage or flux, increase stored energy for constant coil current or mmf, and decrease reluctance or increase inductance.

3.3 Mechanical Model.

The dynamic behavior of the translational mechanical system may be expressed by employing Newton's law of motion. Hence,

$$F_e = m\frac{d^2x}{dt^2} + D\frac{dx}{dt} + K(x - x_0) \tag{12}$$

where F_e is the total magnetic force and m is the mass of armature, while a spring constant and a damping coefficient are represented by K and D, respectively. Parameter x_0 is the value of armature position with the spring neither compression nor tension. For convenience, the damping effect can be neglected here, but the accuracy of analyzing results is acceptable.

3.4. Determination of Electromagnetic Force.

Either λ and x or i and x may be selected as independent variables. Here, let λ and x be selected as independent variables, for a singly excited system such as contactor it is convenient to express the field coenergy as follows:

$$W_c = \int_0^{\lambda} \xi(\frac{1}{L(x)})d\xi = \frac{1}{2} i^2 L(x) \quad (13)$$

where ξ is the dummy variable of integration. Substituting (13) into (11) yields the electromagnetic force which acts to move the armature.

$$F_e = \frac{1}{2} i^2 \frac{dL(x)}{dx} \quad (14)$$

In an ac PM contactor, during closing and opening process, the forced resultant magnetic force is the sum of the electromagnetic part shown in (14) and the permanent magnet part $F_{mag}(x)$. The permanent-magnet force $F_{mag}(x)$ is a function of the armature displacement. In order to simply the control complexity, it is determined by an experimental approach. By application of the Newton's motion law, the motion of armature during closing and opening process is governed by the following formulas:

$$F_e + F_{mag}(x) - F_f = m\frac{d^2x}{dt^2} \quad (15)$$

where F_f represents the tensioned or compressed force of spring systems, for simplicity, it is defined as the only counter force results from the spring systems, but does not include the other forces, for example, friction force.

4 Electronic Control Units

At the opening position, the armature is only forced by a holding force of the permanent magnet. In general, this holding force is insufficient to overcome the spring anti-force and then the armature will be hold at the opening position. However, if the ac PM contactor is energized by an external ac voltage source, for example sinusoidal voltage source, and the equivalent circuit is like Fig. 4(a), an electromagnetic force will be produced due to the generation of coil current and incorporated into the holding force of permanent magnet by a linear approach. The resultant magnetic force is common to be designed large enough to overcome the spring anti-force, therefore, the armature begins moving towards the fixed iron core. After the armature has engaged with the fixed iron core, the coil voltage is removed by the ECU (but not the external ac voltage source). The armature closed with fixed iron core tightly is only forced by the holding force of the permanent magnet. However, since the reluctance in the magnetic circuit is reduced greatly, the holding force should be sufficient to overcome the spring anti-force.

If the external voltage source is cut off or its value is detected by the ECU lower than the maximum releasing voltage, the ac PM contactor begins to open the armature. By applying the reserved breaking voltage across the capacitor C to the contactor, the equivalent circuit of the electrical system is shown in Fig. 4(b). A reverse electromagnetic force is produced due to the coil current flow in the reverse direction. This electromagnetic force is first used to overcome the holding force of the permanent magnet and the remaining force is again combined with spring tension force for opening the contactor as quick as possible.

Fig. 5 shows a complete electronic control circuit, it is referred to as ECU here. As indicated in Fig. 5, ECU is merely composed of some simple digital and analog components. The operation of ECU is determined by the instantaneous voltage across the two terminals of the coil. The designing purpose of the ECU is aimed at breaking or making the proposed ac PM contactor. By taking the energy saving into consideration, the proposed ac PM contactor is only driven by the ECU during closing and opening processes, but does not be driven during holding process. The remainder of this section describes the operation of the ECU. Each functional block shown in Fig. 5 will be described in a separate paragraph.

4.1 Rectifier

Operating from the ac source V_{in}, full-wave bridge rectifier including four diodes D_6~D_8 and an electrolytic capacitor C_1 are equipped with the input of the ECU, as denoted in Fig. 5. It converts the ac source voltage to a ripple-free dc voltage V_o with an average value approximately equal to the peak value of $V_o = \sqrt{2}\ V_m$, where V_m the amplitude of ac voltage source. The value of C_1 is always relatively small. In fact, it is composed by two capacitors in parallel to achieve the correct value for C_1. A metal-

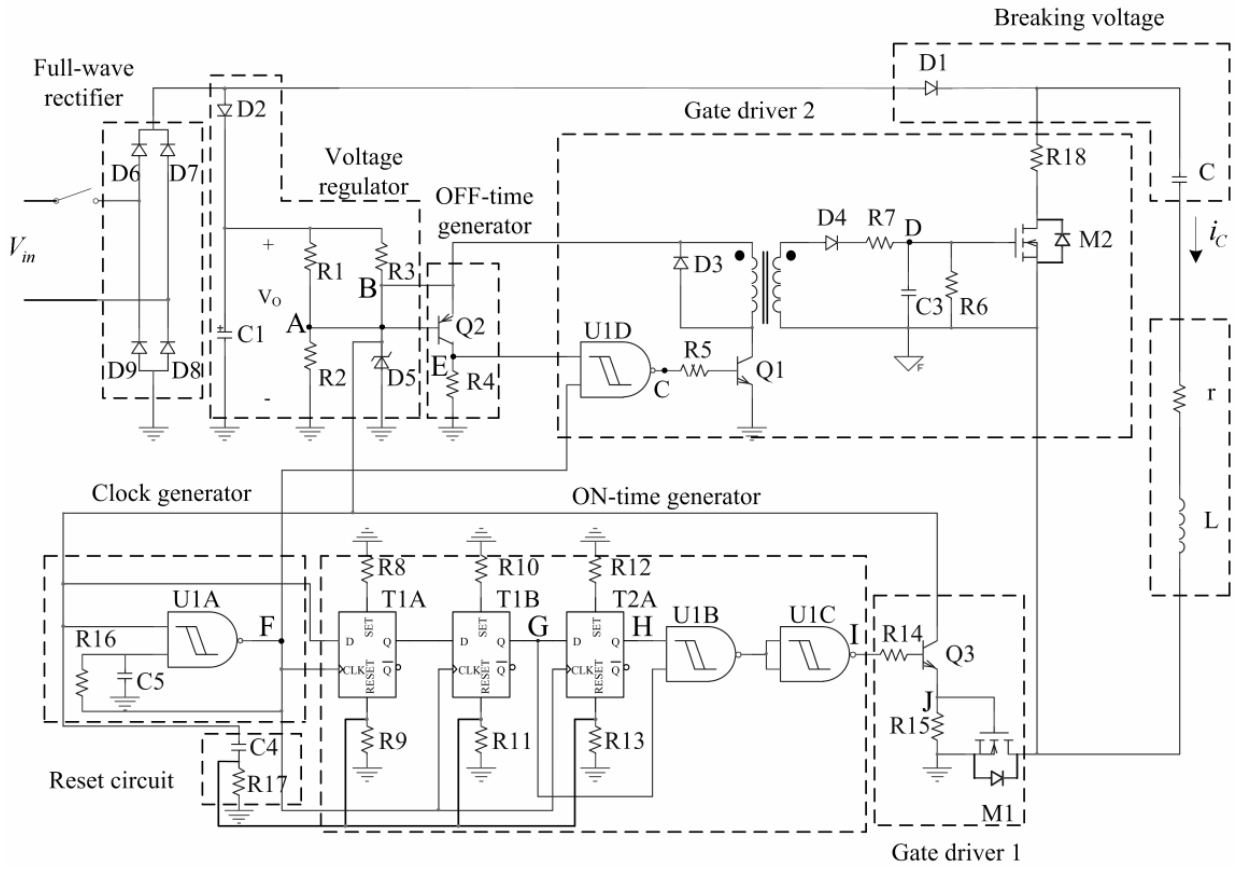

Fig. 5. Schematic circuit diagram of the completed electronic control unit (ECU).

oxide varistor (MOV) (it is not drawn in Fig. 5) is often set across the two terminals of ac voltage source prevents transient ac source over voltages from damaging the ECU of ac PM contactor.

4.2 Voltage Regulator

In addition to the ac voltage source, there are two dc internal power supplies are included in the ECU. As shown in Fig. 5, operating from V_o, the voltage regulator including a resistor R_3 and a zener diode D_5 produces approximately V_{cc}=15 V for powering the electronic control circuits. In contrast, the other one is composed of a capacitor C and reserved a breaking voltage before breaking course begins. When the voltage of ac source is lower than the maximum releasing voltage, the opening process begins working and the breaking voltage across the capacitor is served as the power source of ac PM contactor.

4.3 Gate Driver

There are two power transistors are equipped with the ECU for the making and breaking operation of ac PM contactor. The driving capability related to the signals produced by the ON-time generator and OFF-time generator on the ECU is too weak to directly drive the power MOSFETs. Therefore, these two driving signals are first amplified by the respective gate driver. The gate driver 1 consists of R_{14}, R_{15}, and transistor Q_3 is used to directly amplify the driving signal of MOSFET M1. The gate driver 2 includes many components is used to indirectly amplify the driving signal of MOSFET M2 with an isolated transformer due to the grounding problem.
When the external voltage source is removed, OFF-time generator produces a logically high signal. By switching this signal with the use of a fixed-frequency PWM-modulated signal which is generated by clock generator, this driving signal will be transferred from the primary to the secondary of isolated transformer for the conduction of power transistor M2.

4.4 Clock Generator

For simplicity, it is only composed of a fixed resistor R_{16}, a capacitor C_5, and a NAND-gate U1A. The output of the clock generator is provided with the ON-time generator to act as the reference clock. The on-time count of the power MOSFET M1 is namely based on the frequency of clock generator output. As long as the ac voltage source is present,

the clock generator must be enabled. The output clock frequency f of clock generator depends upon the resistance of the fixed resistor R_{16} and the capacitance of electrolytic capacitor.

4.5 ON-time Generator

In fact, the ON-time generator shown in Fig. 5 consists of a three stages shift register, which includes three D-type Flip Flops, eight resistors, and two NAND gates. As stated in the previously, the calculation of the ON-time is based on the period of the clock output of clock generator. After the external ac voltage source has been established, the ON-time generator is first initiated by a reset signal produced from a reset circuit. All the counting steps of the ON-time generator are listed in Table 1. As the counting number is step 3, namely the outputs of the second and third register are logically high. The ON-time generator outputs a logical high level at this moment and maintains over a period of reference clock. Although the voltage source is still present, it should be reset immediately after a period of reference clock.

Table 1. Truth table of ON-time generator

State	T1A_Q	T1B_Q	T2A_Q
Initial state	0	0	0
Step 1	1	0	0
Step 2	1	1	0
Step 3	1	**1**	**1**

4.6 OFF-time Generator

The OFF-time generator includes a transistor Q_2 and a resistor R_4. The transistor Q_2 acts as a voltage comparator. During closing and holding processes, the base voltage (node A) of transistor Q_2 is bigger than that of emitter (node B) of transistor Q_3, and leads to the voltage across the resistor R_4 is low voltage. When the ac voltage source is removed or the opening process begins, the voltage of node A is smaller than that of node B. Therefore, the transistor Q_2 is conducted and the voltage across the resistor R_4 becomes high voltage. In other words, during opening process, the OFF-time generator produces a logically high level voltage for conducting the power MOSFET M2 to open the contactor.

4.7 Breaking Voltage

The power circuit is shown in Fig. 5 indicates an electrolytic capacitor C is connected with the coil in series. During closing process, the contactor is energized by adding a rectified dc voltage source. The breaking capacitor C is charged through the diode D_1 until the end of closing process. Later, if the opening process begins, the external ac voltage source is removed and the ac PM contactor must rely upon the breaking voltage to supply with the electrical system. As a result of a reverse electromagnetic force is produced by the inverse coil current, the holding force of the permanent magnet is overcome. The armature forced by the spring anti-force and remaining electromagnetic force is again moved back to the initial opening position.

4.8 Reset Circuit

This timing circuit ensures that ON-time generator does not begin operation until the internal control voltage has become stable for a sufficient period time. Capacitor C_4 and resistor R_{17} set the time delay. Before start up, the capacitor C_4 has discharged due to the absence of control voltage. When power is first applied to the electronic control circuit, capacitor C_4 applies logically high level to the "RESET" terminals of the shift register T1A, T1B, and T2A or ON-time generator keeping its output "low". The voltage across the resistor R_{17} drops as C_4 charges. Eventually, as the voltage across C_4 rises to logically high, the ON-time generator is enabled to work.

5 Tests and Discussions

For convenience, an experimental prototype of ac PM contactor with the proposed ECU shown in Fig. 6 has been established in our laboratory. The newly proposed ac PM contactor is allowed to be supplied with a rated rms voltage $220\,V$ of ac voltage source. Contact's capacity is $5.5\,KW$ and the nominal coil current is $24\,A$. The number of windings is 3750 turns, the coil resistance is $285\,\Omega$, and the armature mass is $0.115\,Kg$. The detailed specifications are relevant to the permanent magnet were listed in Table 2. In addition to the experimental prototype was made, the computer simulation model was also setup. In order to verify the correctness of the simulation model, the simulation results were compared with the corresponding experimental results. According to the mathematical models of ac PM contactor developed in the section 3, the computer simulation model was established by using Matlab/Simulink software tool and shown in Fig. 7.

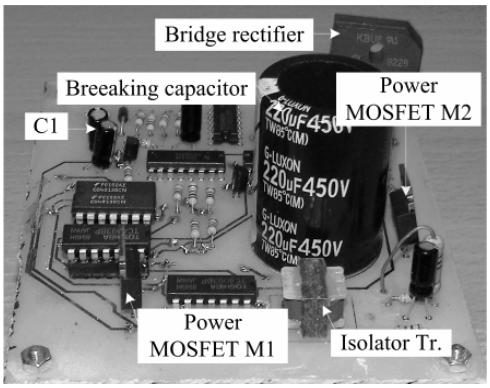

Fig. 6. Shows the completed photograph of the ECU.
Table 2. Specifications of the permanent magnet.

Parameters	Data	Unit
Diameter	10	mm
Width	2	mm
Magnetic flux density	0.137	Tesla
Magnetic field intensity	105	KA/m
Weight	< 1	g

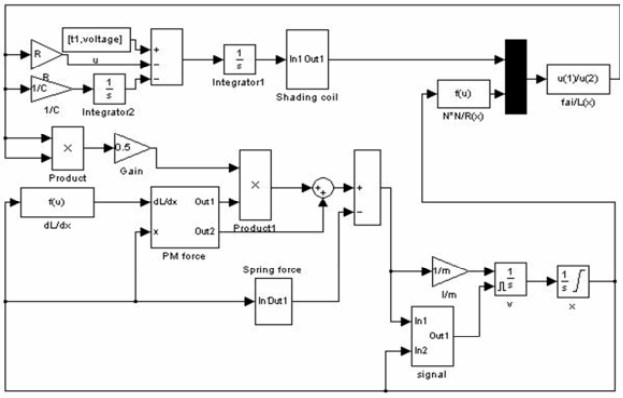

Fig. 7. Sketches the completed simulation model of the proposed ac PM contactor.

5.1 Closing Process

Let an ac voltage source be applied to the coil of the ac PM contactor. First of all, a reset signal is produced by the power-on reset circuit for initiating the output state of ON-time generator. As the ON-time generator is counted from the initial state to step 3, the output of ON-time generator becomes a logically high level. This ON-time signal with logically high level is a one shot and the maintaining time is over a period of reference clock. The logical ON-time signal must be amplified by a gate driver 1 and used to conduct the power MOSFET M1. There is a current i_1 flows through the coil and begins charging the breaking capacitor C. The ac PM contactor is assumed to be applied an ac sinusoidal excitation. Hence, the characteristic behaviors of an ac PM contactor during closing process are to be described by its time-varying coil voltage, armature displacement, and force curves and diagrammed in Fig. 8. The time-varying coil voltage illustrated in Fig. 8(a) depicts that the ON-time period is from $t = 0.015\,\text{sec}$ to $t = 0.07\,\text{sec}$. As a result of the breaking capacitor is connected with the coil in series, the charged braking voltage across the breaking capacitor is increasing that followed by the increase in ON-time. By KVL, the coil voltage attenuates exponentially with time. As the time-varying armature-displacement curve is shown in Fig. 8(b), there is no any armature displacement is produced before time $t = 0.015\,\text{sec}$ because the holding force is insufficient to overcome the spring anti-force. This phenomenon is maintained to the time $t = 0.02\,\text{sec}$ although the ac voltage source is applied to the ac PM contactor at time $t = 0.015\,\text{sec}$. Since the coil current is lagging the coil voltage and gradually increased, the simulated resultant magnetic force shown in Fig. 8(c) which is made of the electromagnetic force and the holding force of permanent magnet begins to overcome the spring anti-force after time $t = 0.015\,\text{sec}$.

In addition, after time $t = 0.07\,\text{sec}$, the coil voltage is cut off. We can see that the armature displacement is not affected by the variation of the coil voltage. When the movable iron core engaged with the fixed iron core, the total reluctance in the magnetic circuit is reduced greatly. To overcome the spring tension force, the force acts on the armature can only rely upon the holding force of the permanent magnet. In addition to little input electrical energy will be absorbed by the electronic control circuit, no any energy dissipation is needed by the contactor body.

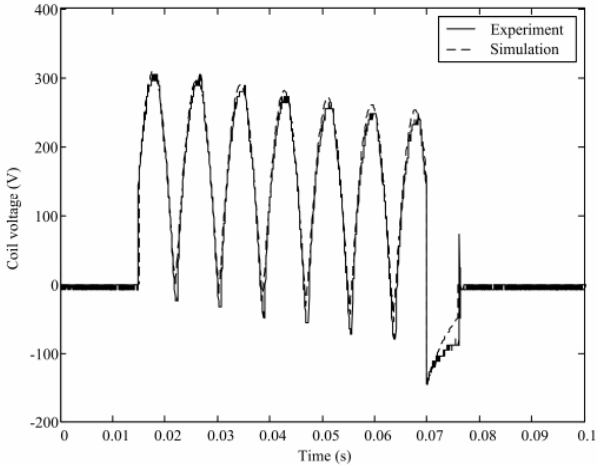

(a)

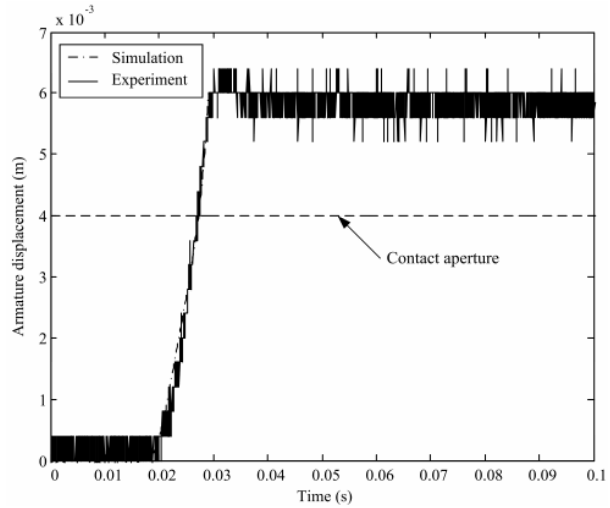

(b)

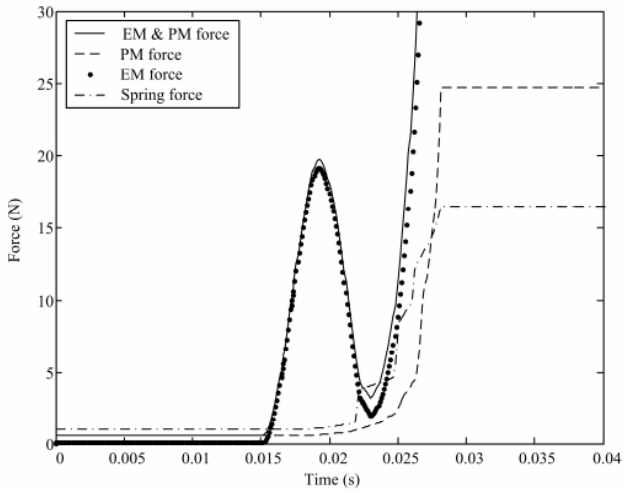

(c)

Fig. 8. Plots the time-varying curves during closing process: (a) coil voltage; (b) armature displacement; (c) forces.

5.2 Opening Process

During opening process, tests on experimental prototype and computer simulation model were carried out and results were diagrammed in Fig. 9. The ac voltage source is removed. To overcome the holding force of the permanent magnet acts on the armature, the voltage across the breaking capacitor C shown in Fig. 9(a) is applied to the coil. Since the initialized breaking voltage is negative voltage for the reference polarity of the coil voltage, thus, the current flow through the coil in the reverse direction and attenuates exponentially. A simulated electromagnetic force indicated in Fig. 9(c) is produced by the negative coil current and used to counteract the permanent-magnet holding force. We note that the remaining magnetic force appears to be lower than the spring anti-force. Fig. 9(b) clearly depicts the armature that is moved back to the opening position after $t = 0.23\text{sec}$. The remaining magnetic force assists with the spring tension force to open the contactor as quick as possible.

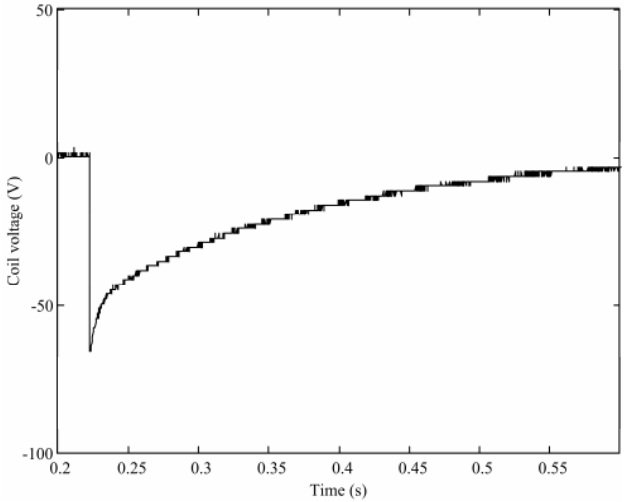

(a)

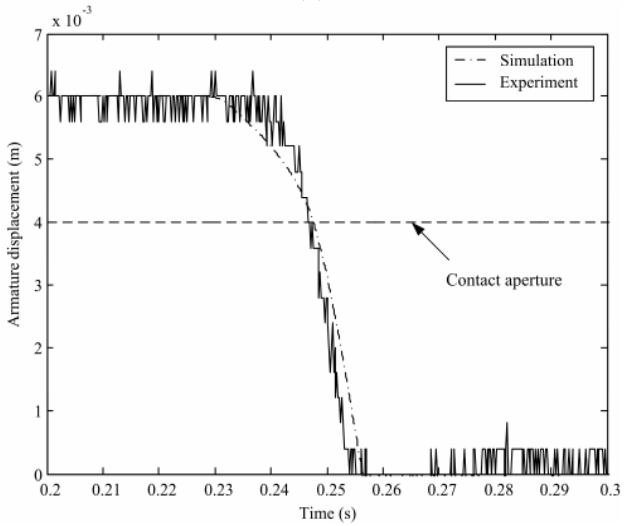

(b)

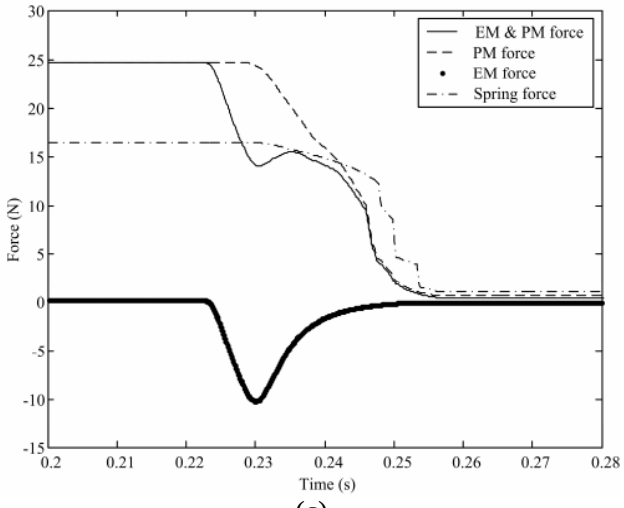

(c)

Fig. 9. Plots the time-varying curves during opening process: (a) coil voltage; (b) armature displacement; (c) forces.

5.3 Assessment of Energy Saving

Testing rigs shown in Fig. 10 aims at measuring the electric energy dissipation of the conventional ac EM contactor and the proposed ac PM contactor over one-year period. In Fig. 10, the coil current flow through the contactor is detected by using an inductive sensor, typed E3N, and based on Hall Effect. The measured coil current is dynamically sampled and recorded by a digital scope. In addition, the coil voltage is also obtained by using a digital scope and an isolated voltage probe. As we known, once above three key parameters related to the power energy calculation, such as the coil current, the coil voltage and the running time interval, are obtained, the energy dissipation during the operation of contactor, of course, is simply acquired. Compared with the testing rig for the measurement of the input electric energy in the conventional ac EM contactor, another one similar testing rig is arranged aims at the measurement of input electrical energy dissipation for the proposed ac PM contactor. Because the inherent characteristic of the newly proposed ac PM contactor, the proposed ac PM contactor including an ECU should be equipped with between the ac voltage and the contactor body. The proposed ac PM contactor is merely energized during closing and opening processes over a short time interval. Normally, the coil voltage of ac PM contactor is completely removed during holding process. Only the ECU dissipates a little electric energy. It is an anticipated result that little energy will be absorbed by the proposed ac PM contactor.

Energy saving characteristic that offered by the proposed ac PM contactor is its superior benefit. As listed in Table 2, both ac PM contactor and ac EM contactor are assumed to be operated in the holding process for one year. The total energy is dissipated by ac PM contactor is only 27% of that by ac EM contactor.

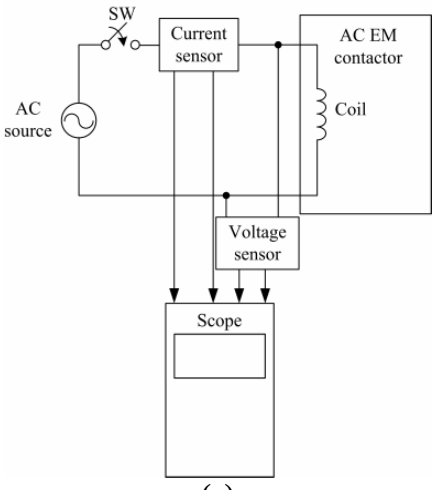

(a)

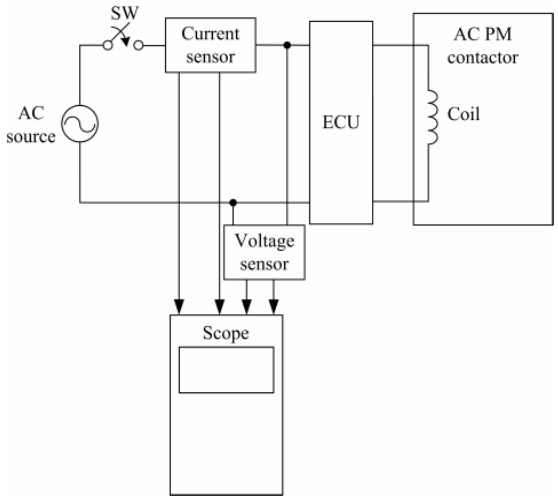

(b)

Fig. 10. Testing rigs for the measurements of electric energy dissipation: (a) ac EM contactor; (b) ac PM contactor.

Table 2. Energy saving comparison between ac EM contactor and ac PM contactor.

Item	EM type	PM type
Voltage (V)	220	220
Coil current (A)	0.079	0.014
Volt-Ampere (VA)	17.402	3.036
Total energy (KWH)	152.441	26.595
Fee (NT dollars)	457.324	79.786

6 Conclusion

A newly permanent magnet ac contactor is proposed in this paper. Compared with the conventional ac EM contactor, an outstanding energy-saving performance is to be achieved. By arranging a permanent magnet on the armature and intervening a hardware-based electronic control unit between ac voltage source and contactor body, during holding stage, almost no energy is dissipated by the contactor body. Only little electric energy is absorbed by the electronic control circuit. The more the running time is, the large amount of energy will be saved. Crucial advantages, such as noise-free at lower voltage, no voltage-sags affections, and their coil will not be burnt due to continual working state, are also obtained. The feasibility and effectiveness are validated through experimental and simulation tests. Testing results show that approximating one-third of the total energy is needed to be dissipated in

the newly proposed ac PM contactor for completing the making and the breaking operations.

Acknowledgment

This work was supported by the National Science Council (Taiwan) under grant NSC 96-2221-E-270-016.

References:

[1] W. Rieder and V. Weichsler, Make Erosion on Ag/SnO_2 and Ag/CdO Contacts in Commercial Contactors, in *Proc. of the 36th IEEE Holm Conf. on Electrical Contacts*, 1990, pp.110–116.

[2] H. Nouri, F. Kalvelage, T. S. Davies, and J. H. Kiely, Erosion Dependency of 3-phase Contactor Contacts on Configuration of Loads, in *Proc. of the 46th IEEE Holm Conf. on Electrical Contacts*, 2000, pp.153–160.

[3] H. Tahara and T. Masuyama, Ground-Based Experiment of Electric Breakdown of Spacecraft Surface Insulator in an Ambient Plasma Environment, *IEEE Trans. on Plasma Science*, Vol.34, 2006, pp.1959–1966, 2006.

[4] T. S. Davies, H. Nouri, and F. Britton, Towards the Control of Contact Bounce, *IEEE Trans. on CHMT*, Vol.19, No.3, 1995, pp353–359.

[5] Q. Licer, N. E. Alarm, and M. Mrabi, Passivity and Energy based Control for Finding Optimal Compass Gaits, *WSEAS Trans. on systems*, Vol. 5, Sep. 2006, pp.2061-2067.

[6] C. T. Chi, A Study of Closing Adaptive Control Electronically Controlled Intelligent **C**ontactor, *TENCON 2006. IEEE Region 10 Conf.*, 2006, pp.1-4.

[7] Y. Liu, D. Chen, L. Ji, and Y. Geng, Dynamic Characteristic and Contact Bounce Analysis for an AC Contactor with PWM Controlled Coil, in *Proc. of the 53rd IEEE Holm Conf. on Electrical Contacts*, 2007, pp.289–293.

[8] A. Carballeria, Erosion Characteristic at Make and Break of Contactor Contacts, in *Proc. of the 11th Int. Conf. Electrical Contact Phenomena*, 1982, pp.175–179.

[9] M. Andriollo, G. Bettanini, G. Martinelli, A. Morini, S. Stellin and A. Tortella, Electromagnetic Design of In-wheel Permanent Magnet Motors, *WSEAS Trans. on Power Systems*, Vol. 1, Feb. 2006, pp. 303-310.

[10] H. Manhart and W. Rieder, Erosion Behavior and Erodibility of Ag CdO and Ag SnO_2 Contacts under AC3 AND AC4 Test Conditions, *IEEE Trans. on CHMT*, Vol.13, 1990, pp.56–64.

[11] H. Nouri, N. Larsen, and T. S. Davies, Contact Bounce Simulation Using Matlab, in *Proc. of the 43rd IEEE Holm Conf. on Electrical Contacts*, 1997, pp.284 – 288.

[12] H. Nouri, T. S. Davies, and J. Bruns, Studies into the Possibilities of Devising a Technique for the Measurement of Electromagnetic Interference in Contactor Contacts, in *Proc. of the ICECT*, 1999, pp.317–324.

[13] X. A. Morera and A. G. Antonio, Modeling of Contact Bounce of AC Contactor, in *Proc. of the 50th Int. Conf. on Electrical Contacts*, Vol.1, 2001, pp.174–177.

[14] S. Tan, D. G. Chen, and F. Tao, Intelligent AC Contactor with Feedback Control, *Low Voltage Apparatus*, No.2, 2005, pp.3-5.

[15] Y. Liu, D. Chen, L. Ji, and Y. Geng, Dynamic Characteristic and Contact Bounce Analysis for an AC Contactor with PWM Controlled Coil, in *Proc. of the 53rd IEEE Holm Conf. on Electrical Contacts*, 2007, pp.289–293.

[16] W. Li, J. Lu, H. Guo, and X. Su, AC Contactor Making Speed Measuring and Theoretical Analysis, in *Proc.of the 50th IEEE Holm Conf. on Electrical Contacts*, 2004, pp.403–407.

[17] X. Zheng, Z. H. Xu, and P. M. Zhang, Analysis and Implementation of Zero-Current Breaking Adaptive Control in Intelligent AC Contactor, *Advanced Technology of Elect. Engineering and Energy*, Vol.24, No.3, 2005, pp.77–80.

[18] S. Fang and H. Y. Lin, Magnetic Field Analysis and Control Circuit Design of Permanent Magnet Actuator for AC Contactor, in *Proc. of the 8th Int. Conf. on Electrical Machines and Systems*, Vol.1, 2005, pp.280–283.

[19] M. G. Vanti, A. Raizer, and J. P. A. A. Bastos, A Magnetostatic 2D Comparison of Local Error Estimators in FEM, *IEEE Trans. on Magnetics.*, Vol.29, 1993, pp.1902–1905.